Chapter 2
Methodology

This chapter composes the details on generating two sets of modeled data containing primary and seafloor multiples using a modeling software, verifying the modeled data, testing the sensitivity of parameters used in predictive deconvolution on PTTEP in-house processing software, enhancing periodicity of multiple, and removing them by predictive deconvolution (*PDC*) filter. The optimum criteria that obtained from processing of modeled data were again examined by using real data. The methodology in this research is illustrated in Figure 2-1.

2.1 Forward modeling stage

2.1.1 Generating modeled data

To obtain the modeled data, a two-layer and a three-layer models regarding the geologic model of shallow-hard seafloor are specified to the modeling software accompanied with their acquisition and computation parameters as shown in Table 2-1. Subsequently, both input models are simulated by the modeling software and therefore two modeled shot records are produced in Figure 2-2 and Figure 2-8.

2.1.2 Verifying the modeled data

Verifying the qualification of the two-layer modeled shot was first carried out before any processing work which included *spectral* and *arrival time analysis*.

Spectral analysis of the two-layer modeled shot is illustrated in Figure 2-3. It can be seen that the frequency content was dominant at 30 Hz while the signal of multiples is significantly repetitive from 0.1 to 0.8 second. In addition, plot of its semblance in Figure 2-4 particularly shows a velocity trend of multiple, V = 1,500 meter/second, which is constant from upper to lower time.

Arrival time analysis was performed by (1) predicting several possibilities of raypaths that can be generated from the input model in Figure 2-2 (a) as shown in Figure 2-5, (2) calculating 2-way travel time curves of those ray paths, (3) plotting those curves in Figure 2-6, and (4) comparing the calculated 2-way travel time curves with several hyperbolae in the modeled shot on the same scale in Figure 2-7. The comparison shows that arrival times of seismic events versus offsets of both figures are well matched, thus seismic events in the modeled shot can be classified and refered to the name of the raypaths previously labeled in the Figure 2-6.

Verifying the qualification of the three-layer modeled shot, in Figure 2-8, was later conducted which followed all procedures of the two-layer modeled data. Spectral analysis of the three-layer shot is illustrated in Figure 2-9. Its semblance plot is exhibited in Figure 2-10 whereas overlay plot of modeled and calculated shot is presented in Figure 2-11. The analysis shows the same results as of the two-layer modeled data.

As verified, it has been found that spectral analysis of both models contains several events of primary and multiple while the trend of multiple velocity constantly exists in both semblances. Moreover, an agreement of arrival time versus offset seen on their overlay plots supports that pulse of wave is generated and propagated through the input models based on wave propagation theory. For these reasons, it can be accepted that both

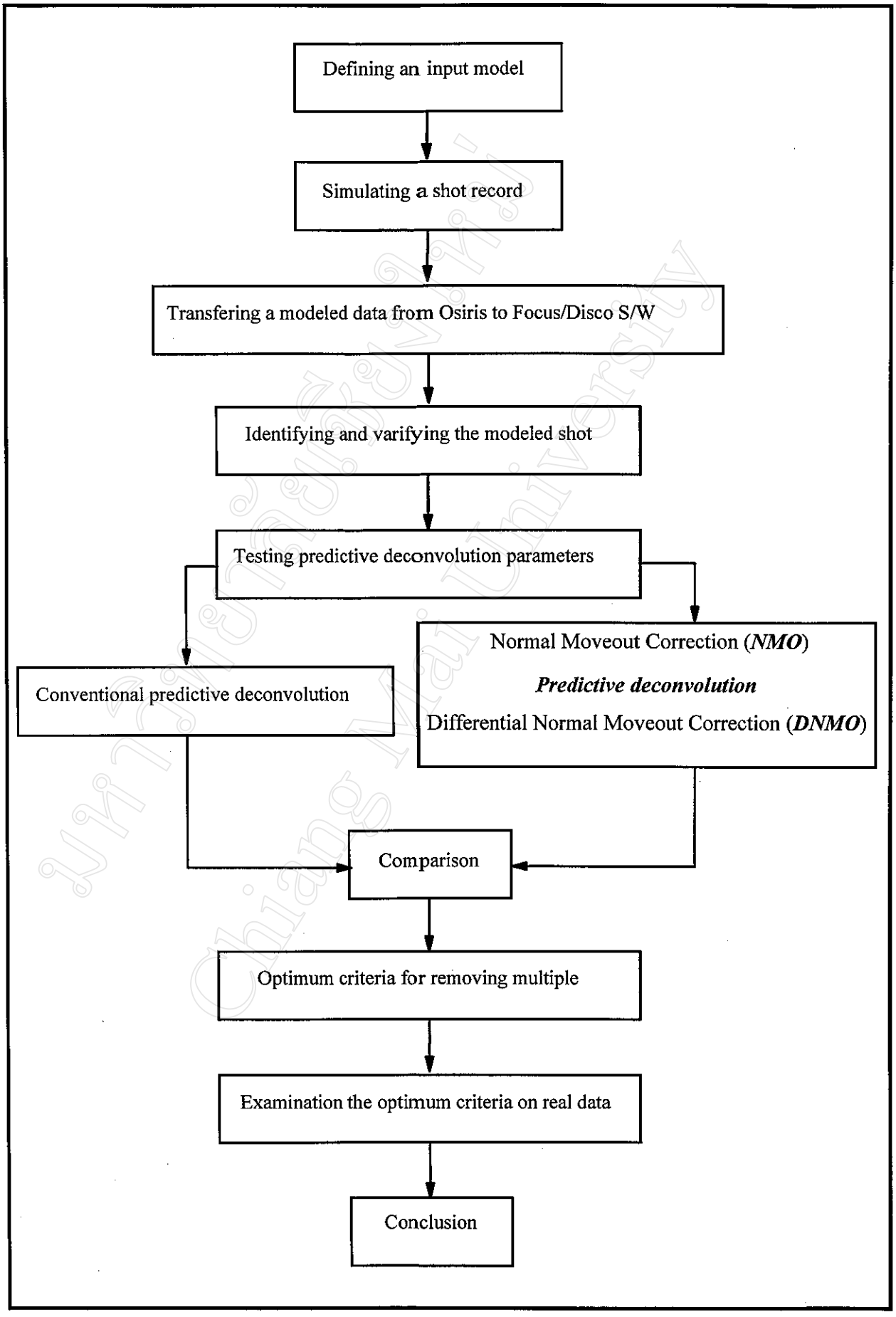

Figure 2-1 Methodology.

Table 2-1 Acquisition and simulation parameters of input models.

Options	Parameters used	Remark
Input file name	Osiris35.pre	Osiris20.pre
Model	Acoustic model	Acoustic model
Layer	***2 horizontal strata***	***3 horizontal strata***
Source		
Type	Point source with Ghost	Point source with Ghost
Depth	10 m	10 m
Receiver	Hydrophone	Hydrophone
Response	Stress	Stress
Lay out	Horizontal seismic profile	Horizontal seismic profile
Depth		
Minimum depth (m)	10 m	10
number of streamer	1	1
Step	10 m	10
Ranges		
Near-offset	10 m	10
Number of recording channel	60	48
Shot interval	10 m	10
Simulation option		
Computation domain	Time	Time
Wave propagation	2 Dimension	2 Dimension
Anti-aliasing	On	On
Spectral sampling adjustment	On	On
Direct wave computation	Integrated	Integrated
Direct wave	Include	Include
Adaptive integration	On	On
Tapering of Kernel	On	On
Low frequency cutoff	Off	Off
Output format	ASCII	ASCII
Kernel output	On	On
Dispersion correction	No	No
Bessel correction	Bessel	Bessel
Computation domain		
Domain definition	Time	Time
Frequency		
Lower frequency	0 Hz	0 Hz
Upper frequency	87.5 Hz	87.5 Hz
Delta frequency	0.1 Hz	0.1 Hz
Center frequency of wavelet	30 Hz	30 Hz
Time		
Lower time	0 sec	0 sec
Upper time	5 sec	5 sec
Delta time	0.004 sec	0.004 sec
Phase velocity for integration		
Integration control	Auto	Auto
Maximum phase velocity	$1x10^9$ m/s	$1x10^9$ m/s
Minimum phase velocity	100 m/s	100 m/s
Number of integral point	900 point	900 point
Accuracy level	medium	medium
Integration control	Automatic	Automatic
Accuracy level	Medium	Medium
Global Epsilon	0.001	0.001
Stop Epsilon	$1x10^6$	$1x10^6$
Local Epsilon	.001	.001
Output file name	Osiris35.out	Osiris20.out

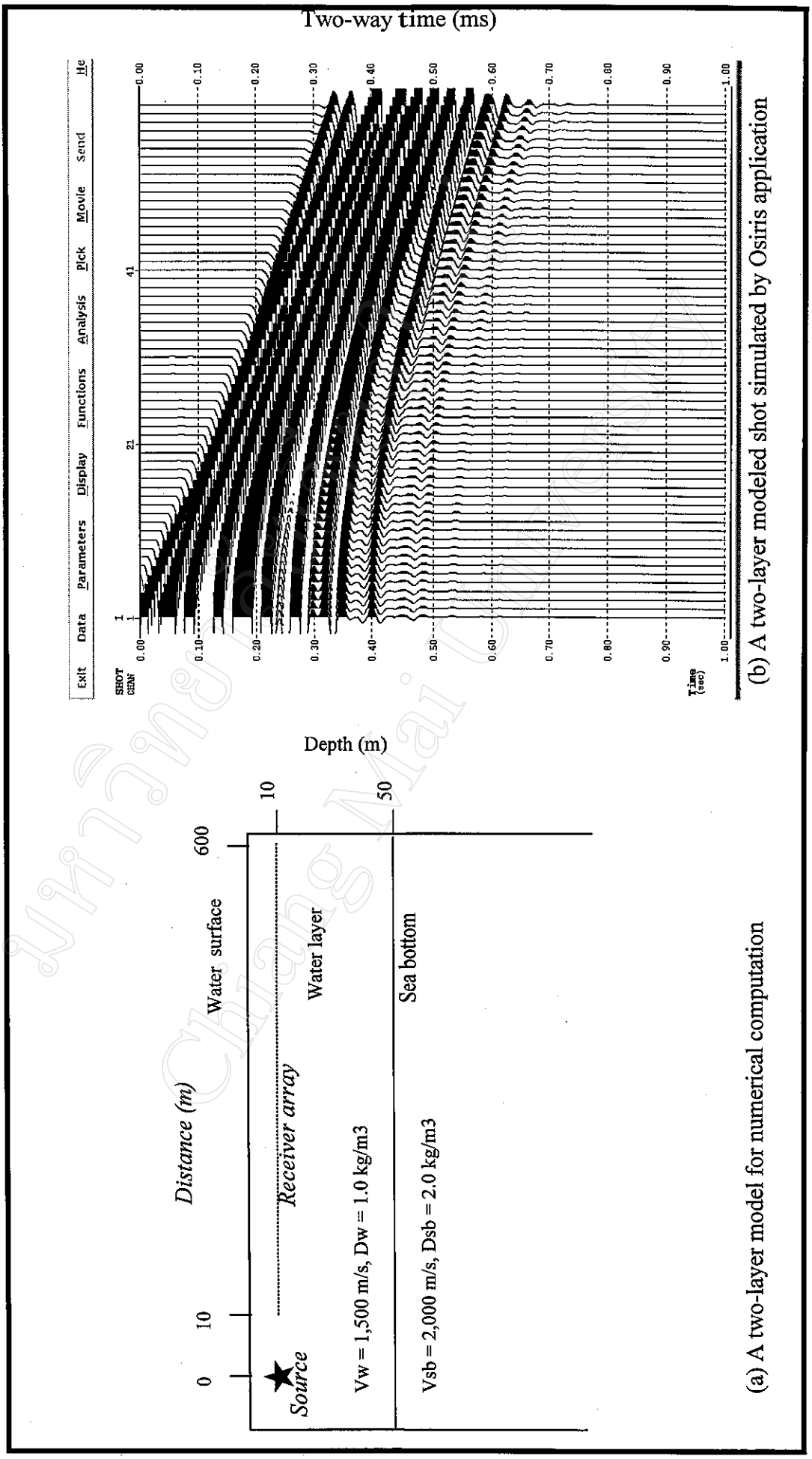

Figure 2-2 Marine acquistion simulation of two-layer model.

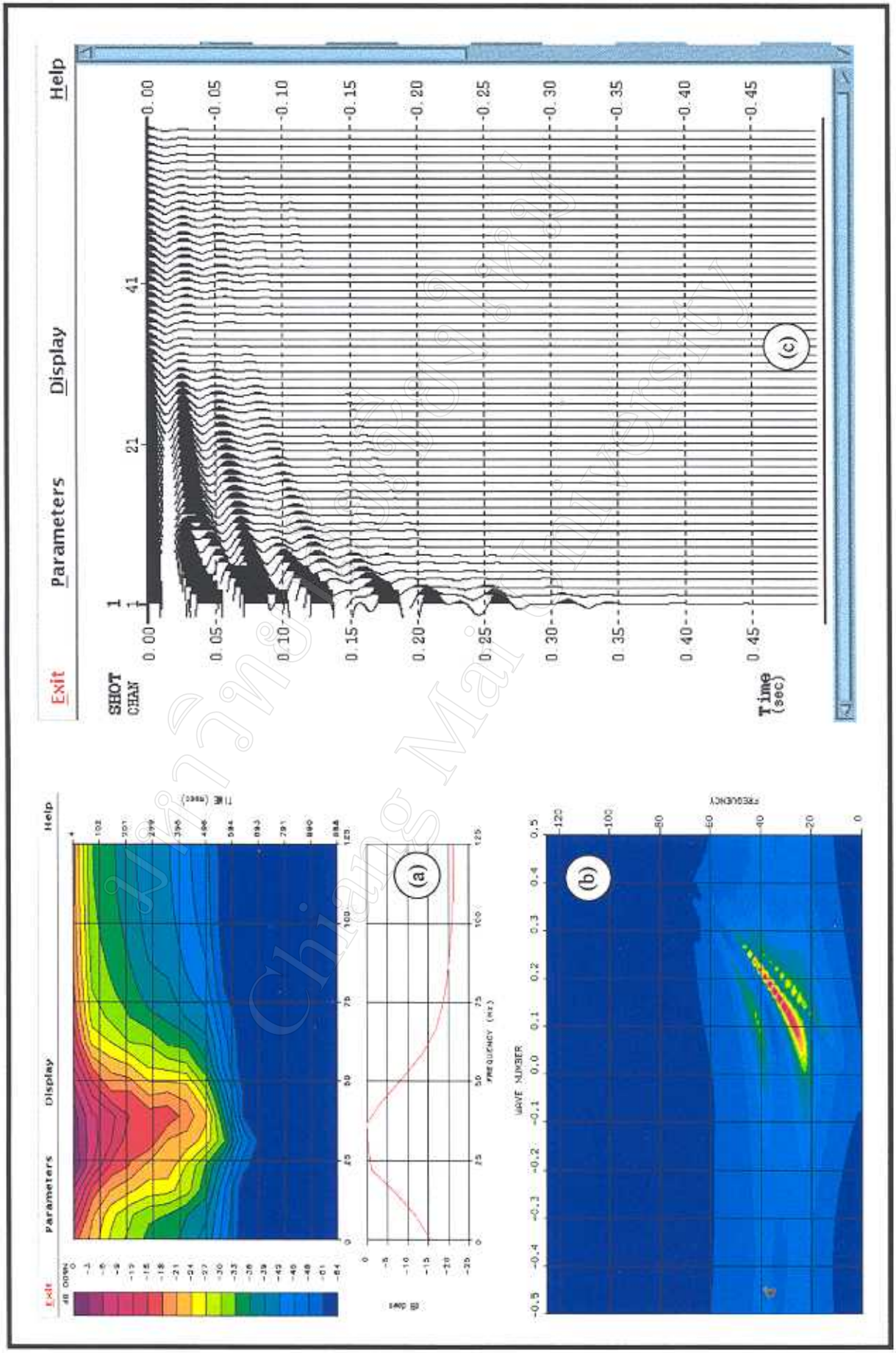

Figure 2-3 Spectral analysis of two-layer modeled shot.
(a) Amplitude spectrum. (b) *F-k* spectrum. (c) Autocorrelation.

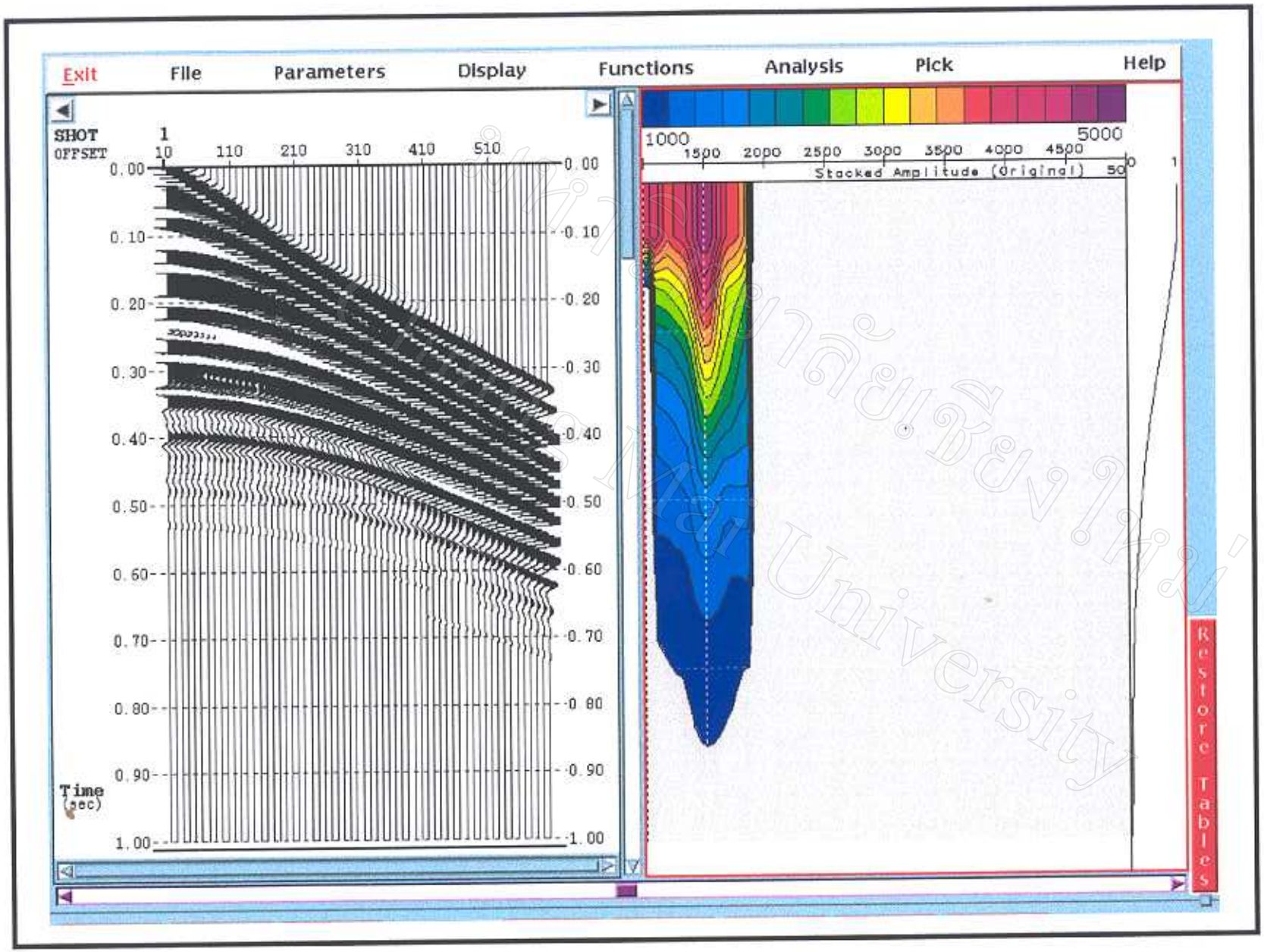

Figure 2-4 Two-layer modeled shot (left) with its corresponding semblance analysis (right).

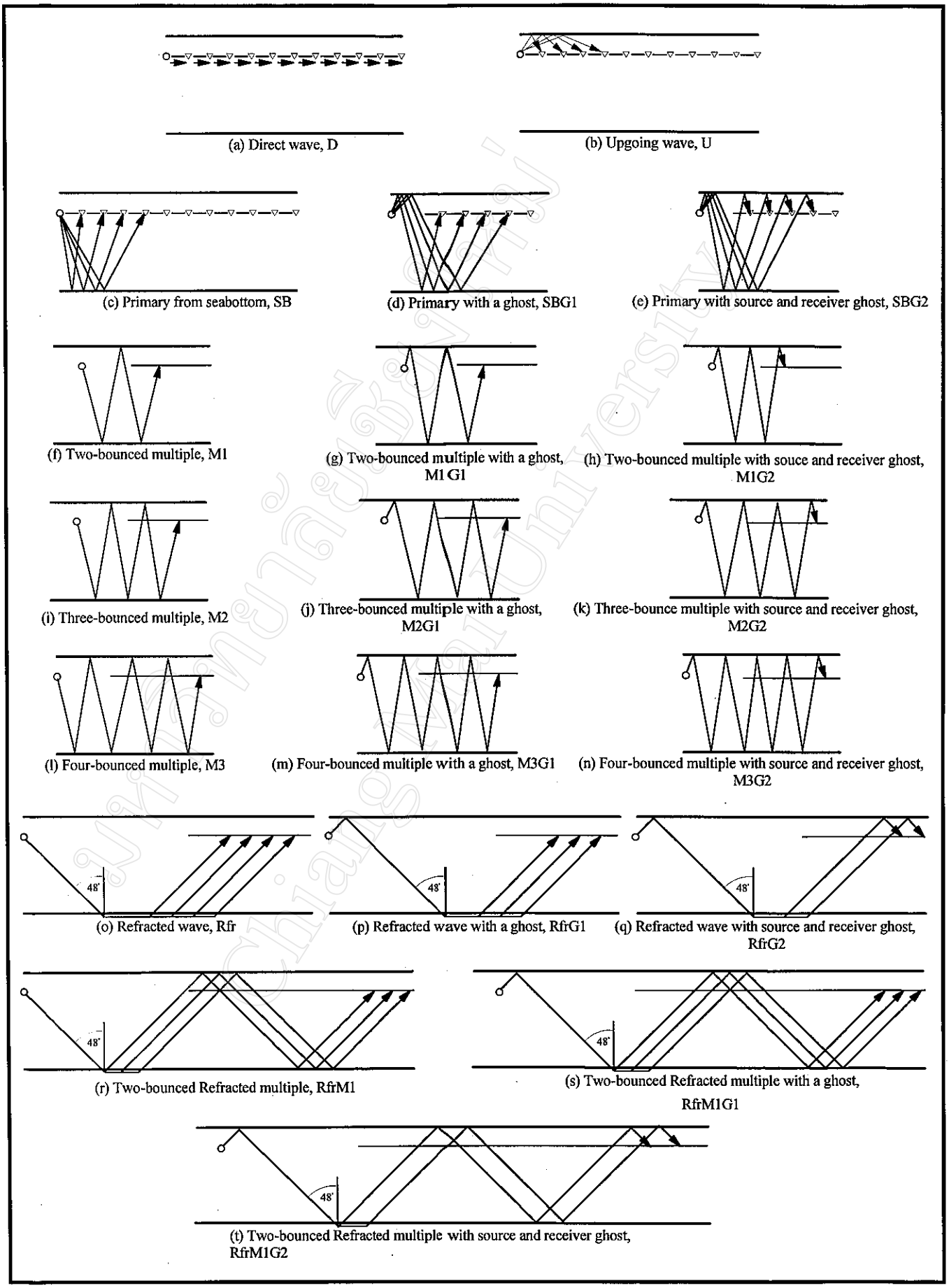

Figure 2-5 Possibilities of seismic events predicted from two-layer input model.

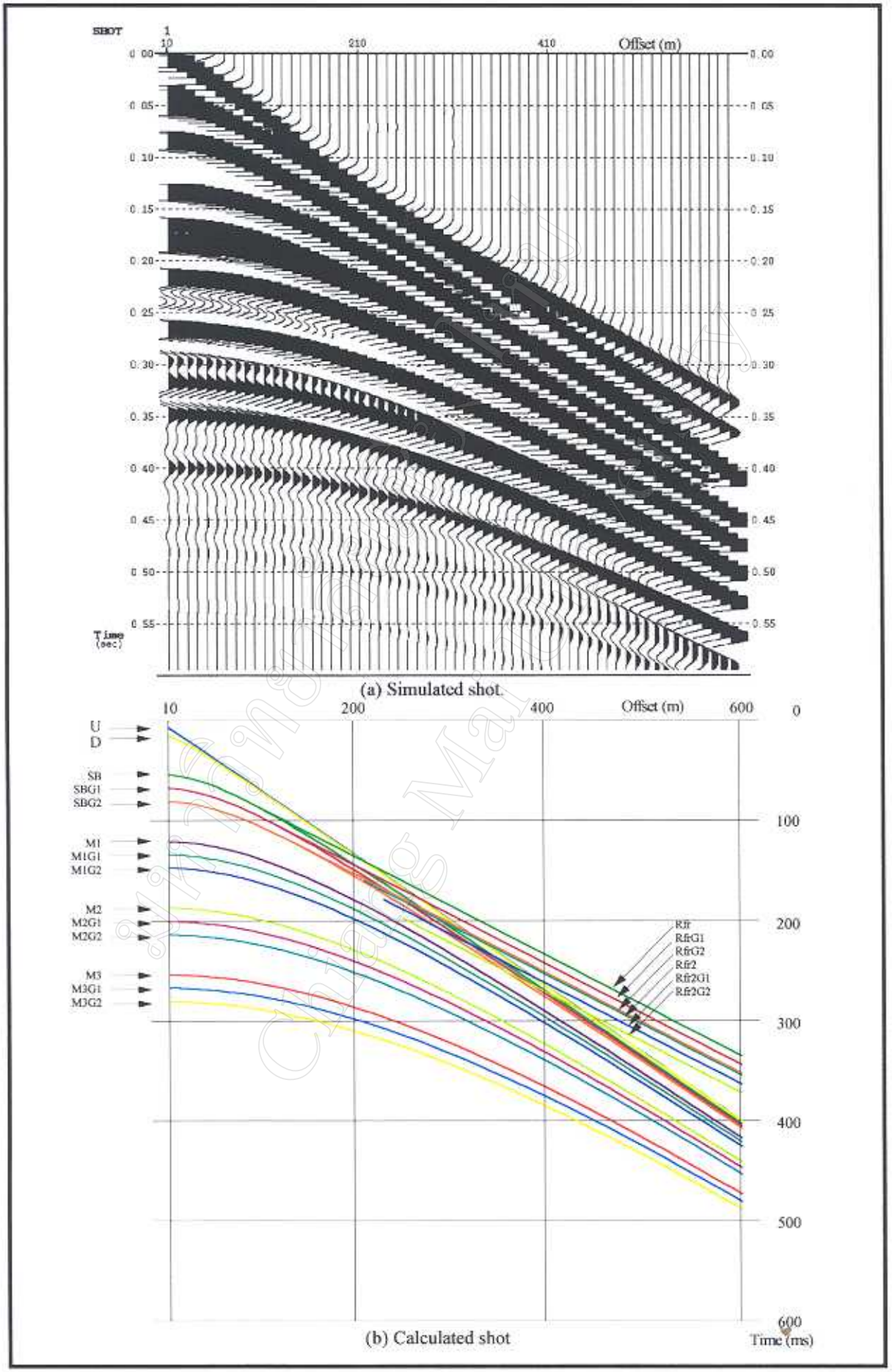

Figure 2-6 Two-layer modeled shots
U = upging wave, D = direct wave, SB = Sea bottom, G = ghost,
M = multipl in order, and Rfr = refracted wave

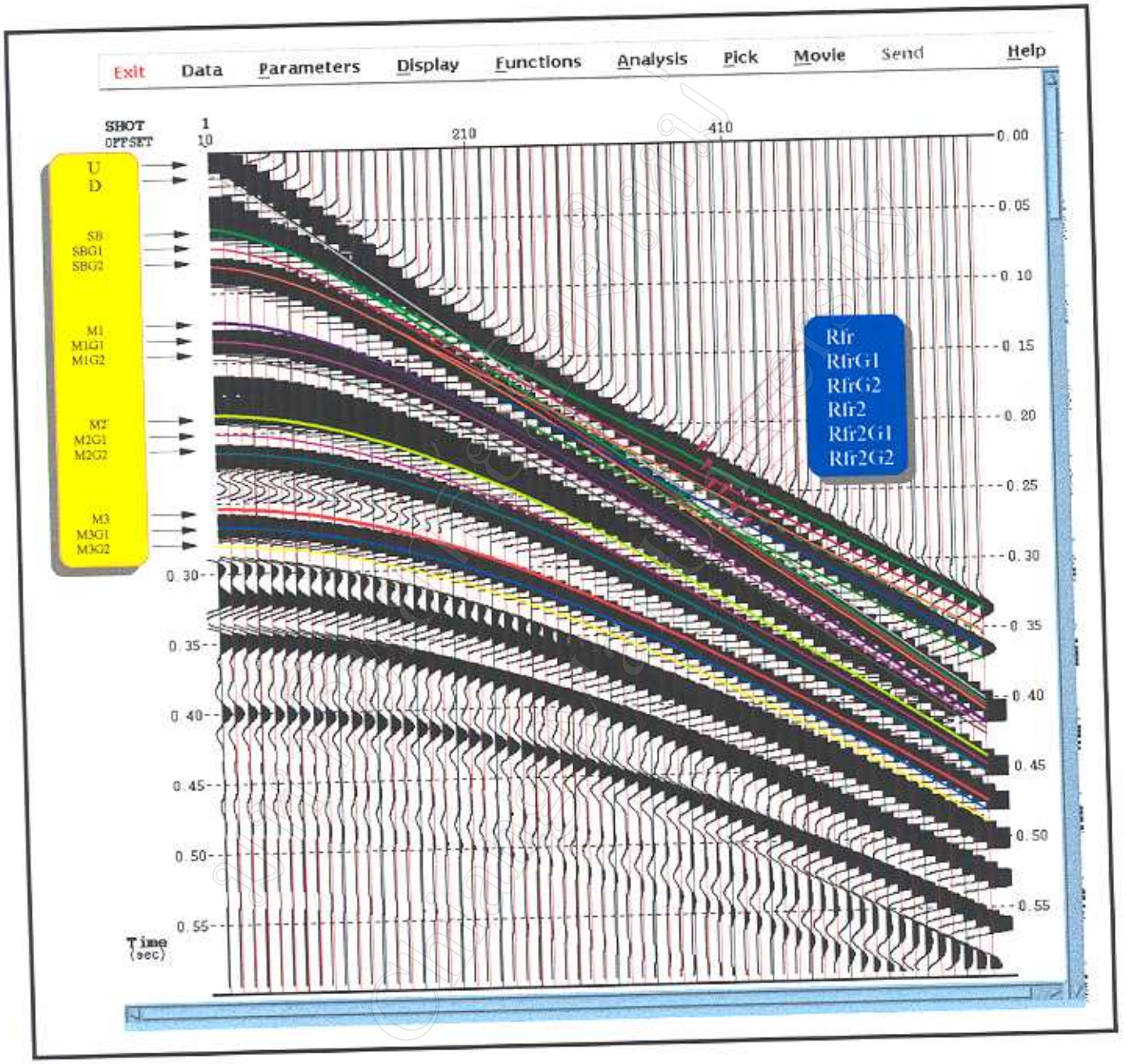

Figure 2-7 Two-layer modeled shot overlaid by calculated shot.
U = upging wave, D = direct wave, SB = Sea bottom, G = ghost, M = multipl in order, and Rfr = refracted wave.

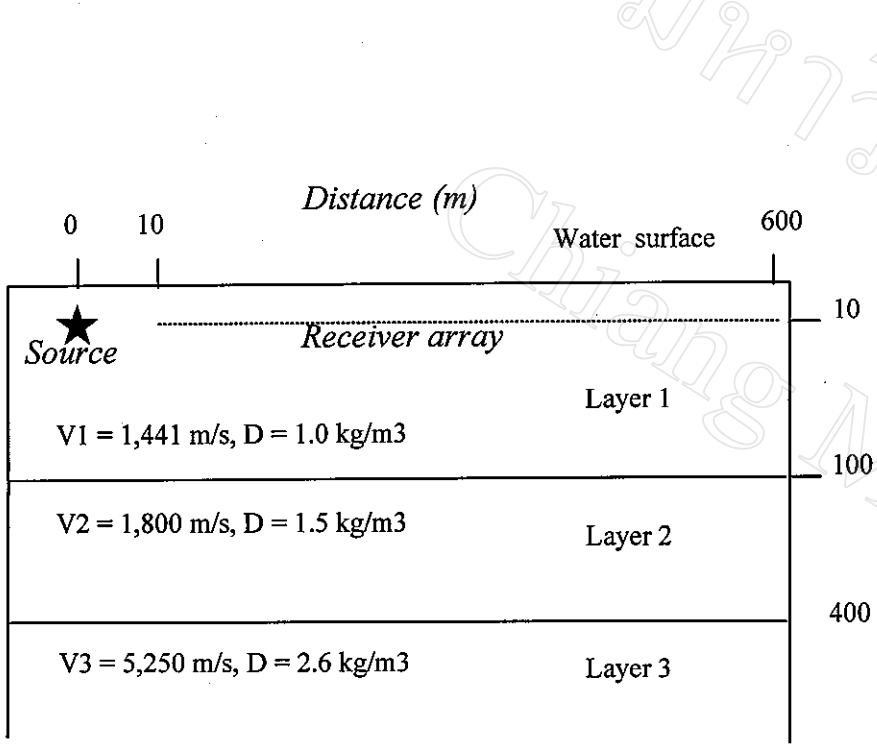

(a) A three-layer model for numerical computation.

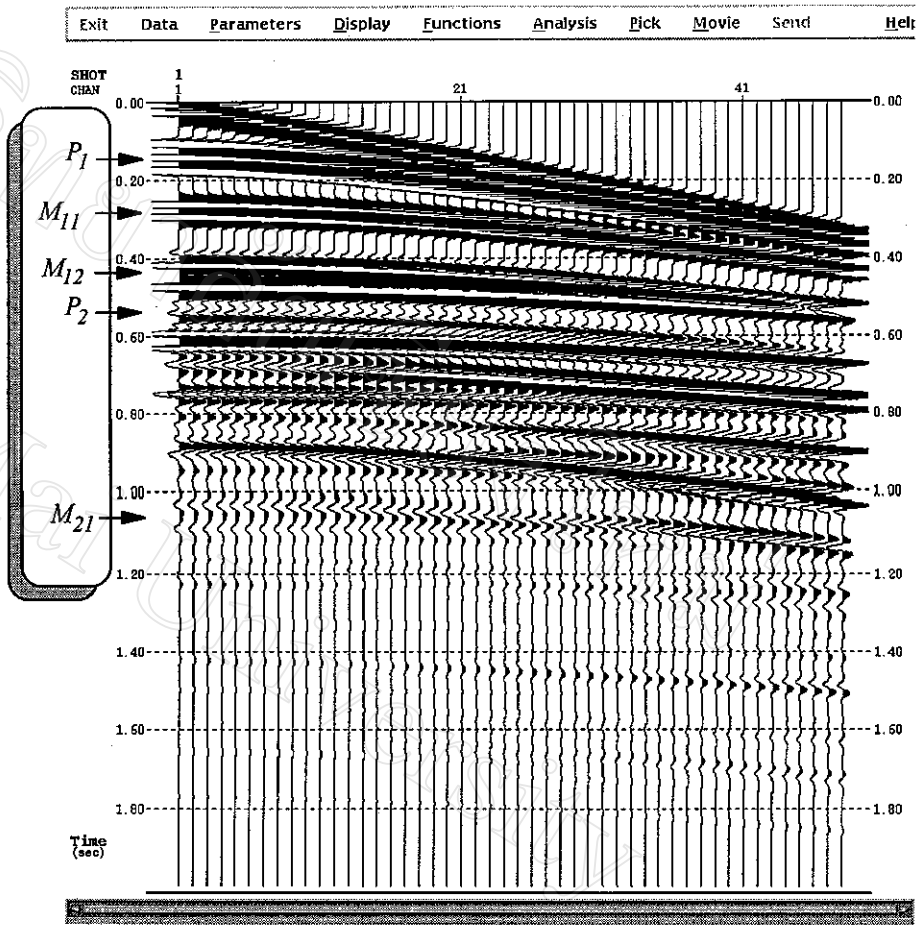

(b) A three-layer modeled shot simulated by Osiris application

Figure 2-8 Marine acquistion simulation of three-layer model. P = Primary,and M = Multiple. The first subscripted indicates layer. The second subscript indicates order of multiple.

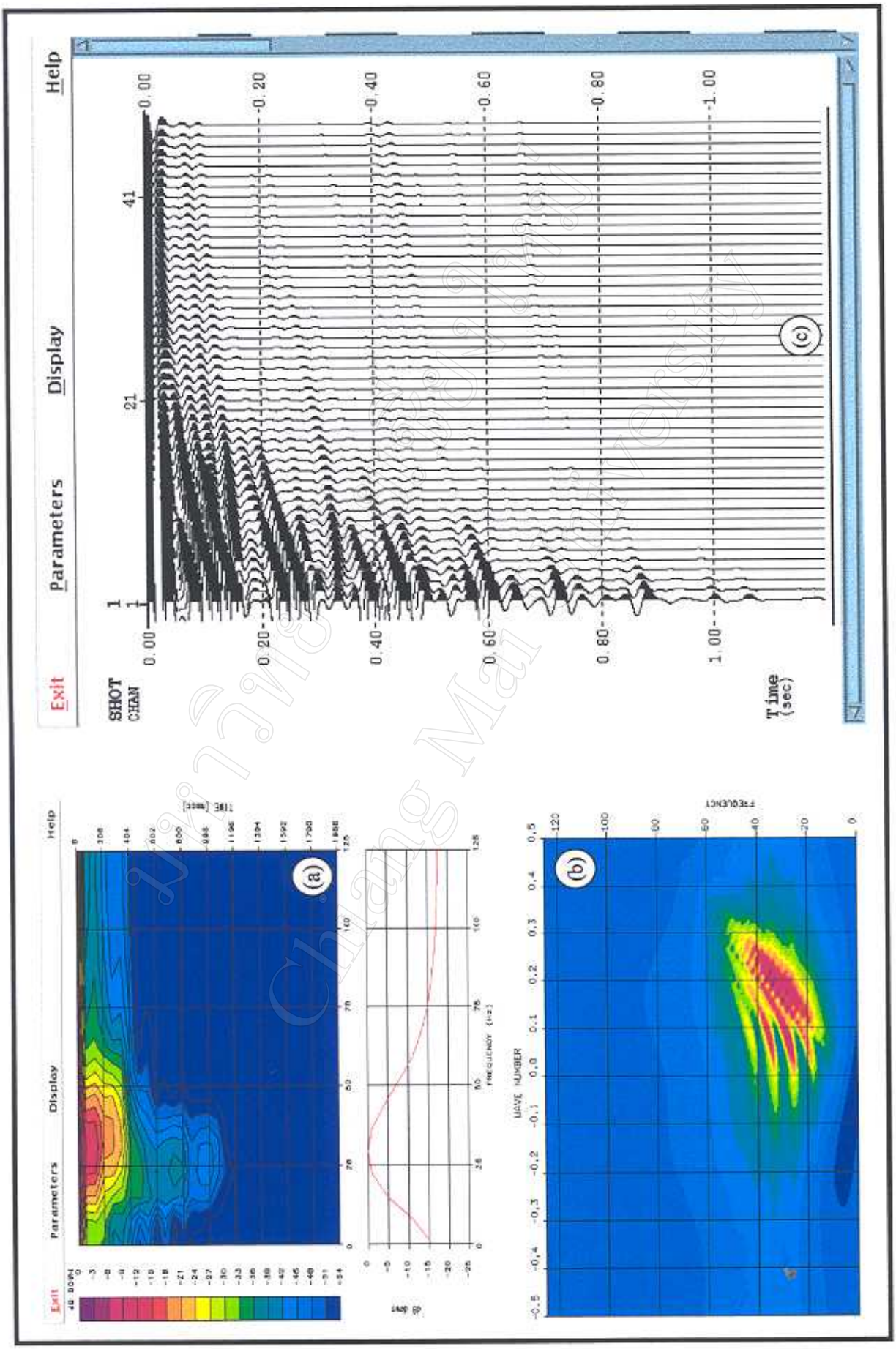

Figure 2-9 Spectral analysis of three-layer modeled shot
(a) Amplitude spectrum (b) F-k spectrum (c) Autocorrelation

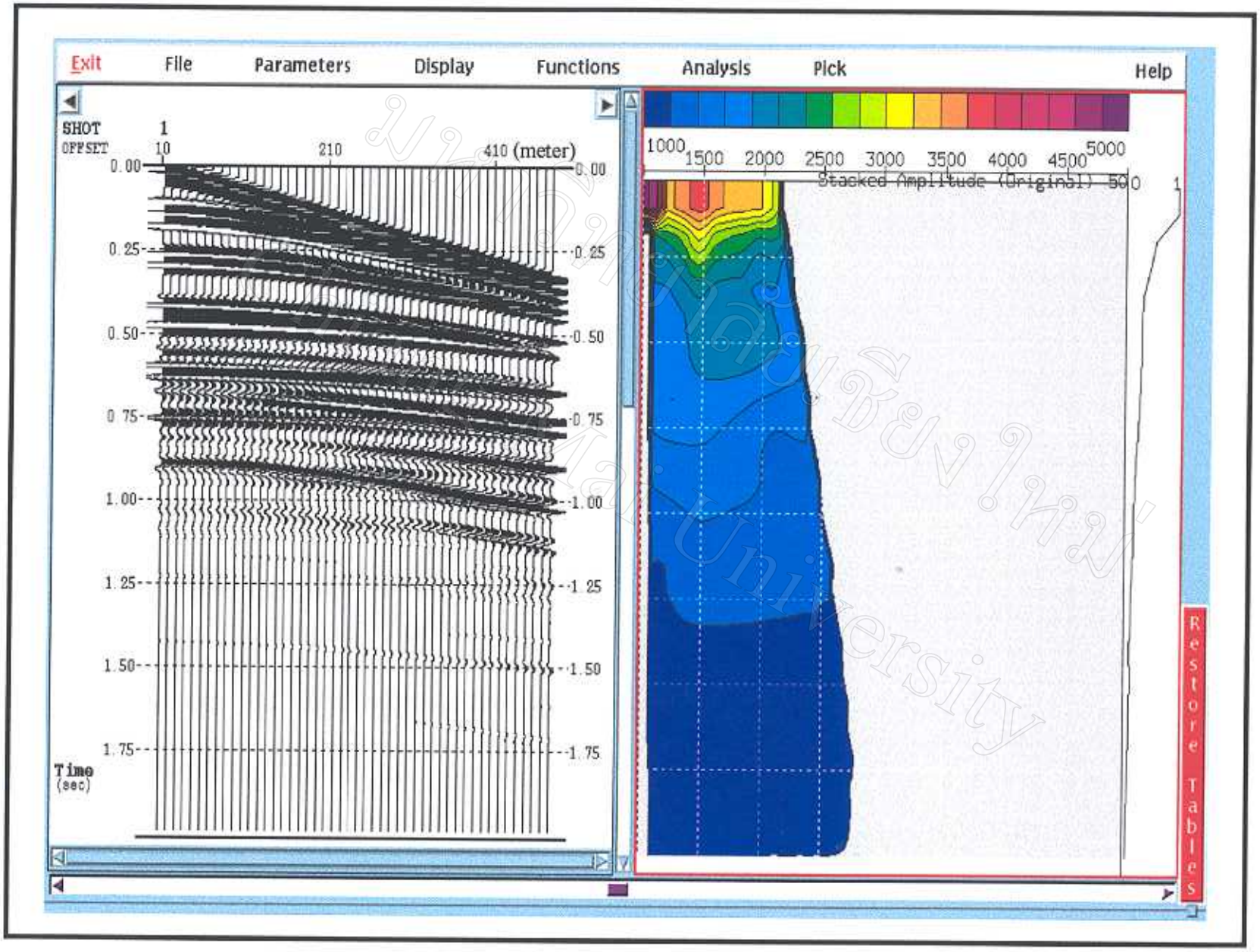

Figure 2-10 Three-layer modeled shot (left) and its corresponding semblance analysis (right)

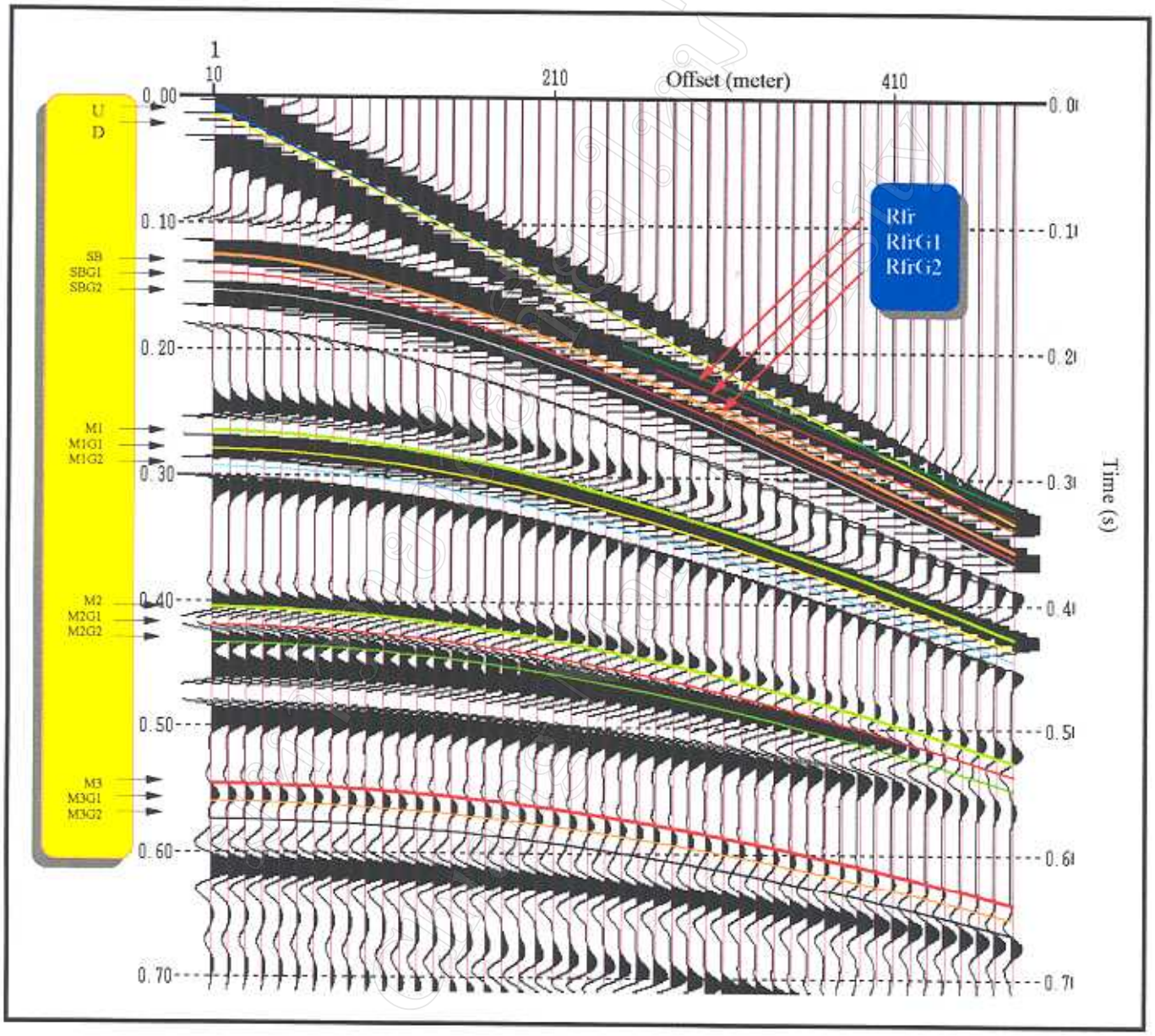

Figure 2-11 Three-layer modeled shot overlaid by its calculated shot.
U = upgoing wave, D = direct wave, SB = primary of sea bottom,
G = ghost, M = sea bottom multipl in order, and Rfr = refracted wave.

modeled shots have adequate quality to be used as the input for data processing in next stage.

2.2 Processing of modeled data

In this stage, the two-layer modeled data was prepared to meet the conditions suitable for processing tests in this study. *Firstly*, the original two-layer modeled shot in Figure 2-2 (a) shows too strong amplitudes at near offset crossing over adjacent traces possibly due to modeling artifacts, so the first three near-offset traces were excluded. *Secondly*, a high-pass filter accompanied with a minimum-phase operator was later applied to change seismic data to be a minimum-phase waveform. This provides the optimum condition for deconvolution (Assumption 5 in Appendix C). *Thirdly*, front-end mute was examined, results of which can be seen in Appendix D (Figure D-1 and -2, respectively). *Fourthly*, Normal moveout (*NMO*) correction, whose algorithm is non linear, was carefully checked its effect which can be observed in Appendix D (Figure D-3 to Figure D-6). Afterwards four main deconvolution parameters namely, autocorrelation gate (G), operator length (n), gap length (α), and prewhitening percentage (ε), were therefore next tested by trial-error method, for details sees Appendix E. It can be noted that although the two- and three-layer modeled shots were created by the same procedure but only the two-layer model shot as initiated from simple model is used to deal with module and parameter testing in Appendix C, D, and E.

The main experiment suggested in this research (Figure 2-1) includes applying *NMO* correction using velocity of multiple to move all curvatures of sea-bottom multiples up to horizontal lines, thus enhancing their periodicity at all offset range, filtering the multiple out, and then removing *NMO* effect (*DNMO*). In filtering step, predictive (*PDC*) deconvolution is applied to the data. By so doing, optimum parameters of designing operator obtained from trial-error tests in Appendix E are exhibited as deconvolution parameters and kept constant throughout the whole experiments carried out on the modeled data. *Lastly*, a band-pass filter with a zero-phase operator is employed to remove high frequency noise normally generated from deconvolution process.

For comparison, a modeled shot with no deconvolution, a shot with conventional *PDC* without periodicity enhancement technique are also performed in a like manner. Flow of processing sequence of three different cases is shown in Table 2-2. Consequently, results of the experiments in common shot gather are compared to see which sequence yields better multiple removal results. Note that both of two- and three-layer model data are passed through the flow of sequence in Table 2-2 by the same procedures.

2.3 Processing of real data

To evaluate the optimum criteria of deconvolution, two data sets of seismic survey line acquired over two areas of shallow seafloor were partially selected as test lines of conventional and new technique. Details of acquisition parameters are illustrated in Table 2-3. Processing of real data needs the same conditions as applied on the modeled data, however, in practical details, some additional applications may require. Both sets were therefore processed with both the new and the conventional methods to confirm the parameters obtained from processing of the modeled data. In addition, to ensure that the package of *PDC* should work well in common shot gather (*CSG*), a raw shot record form each sets was early selected and tested the ability of both the conventional and the new

Table 2-2 Flow of processing sequences of modeled data

Raw shot with no deconvolution	Conventional *PDC*	Periodic Enhancement before *PDC*	Remarks
Input	Input	Input	Modeled shot
Trace Editing	Trace Editing	Trace Editing	Killing first 3 near traces
Filtering	Filtering	Filtering	Desired output minimum phase
		NMO	V=1,500 m/s for two-layer and 1,441 m/s for three-layers data
Front-end mute	Front-end mute	***Front-end mute***	Under first-break zone
		PDC	α *24 ms*, n = 164 ms, ε = 0.1 %, G = 1,000 ms
		DNMO	V=1,500 m/s for two-layer and 1,441 m/s for three-layer data
Output	Output	Output	

PDC = Predictive deconvolution : *NMO* = Normal movout correction : *DNMO* = Differential *NMO* correction

α = Gap distance : n = Gap length : ε = Prewhitening percentage : G = Autocorrelation gate

Table 2-3 Acquisition parameters of two seismic data sets in this research.

(Courtesy PTTEP)

Acquisition		*Data set 1*	*Data set 2*
	Data shot by	Digicon	Geco-Pakla
	Vessel	Ross seal	M/V Geco Saphire
	Date of survey	Aug/Oct 1994	
Cable			
	Streamer type	DSS 240 Digital	Nessie 4
	Length	3115 m	3119 m
	No. of groups	240	240
	Group interval	12.5 m	12.5 m
	Streamer depth	4 - 8 m	5 m
Source			
	Energy source	Airgun	Bolt airgun
	Volume	2970 Cu in	1354 Cu in
	Pressure	2000 PSI	2000 PSI
	Gun array depth	6 m	5 m
	Shotpoint interval	25 m	37.5 m
	Near-offset distance	226 m	131 m
	Coverage	60 folds	40 folds
Instrument			
	Recording system	DSS 240 Digital	TRIACQ
	Digital tape format	SEG-D	SEG-D
	Tape density	6250 BPI	3590 Catridge
	Low cut filter/slope	3 Hz at 6 dB/Oct	3 Hz at 6 dB/Oct
	High cut filter/slope	160 Hz at 72 dB/Oct	120 Hz at 72 dB/Oct
	Sample rate	2 ms	2 ms
	Record length	6 / 8 sec	5 sec
Navigation			
	Primary	: Multifix GPS	
	Secondary	: Skyfix	

Spread configuration (Inside parenthesis are of data set 2.)

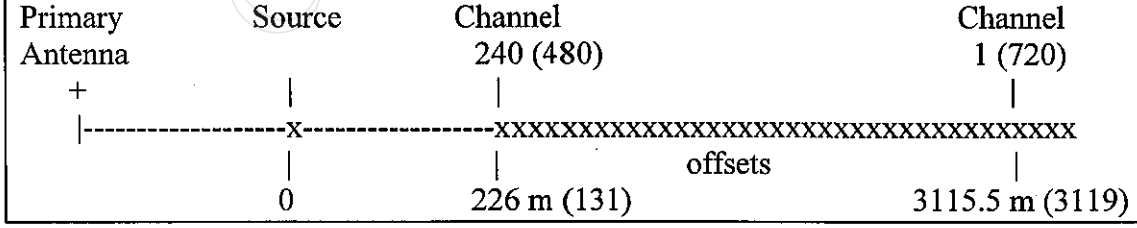

method before sorting all shots to common depth point (*CDP*) gathers. This could be conducted following half of processing sequence in Figure 2-12. Consequently the inspection of results of removing method has been compared in *CSG* and semblance domain in Chapter 3.

Ultimately, raw shots of 2-D seismic data of set 1 and 2 are therefore processed according to the flow of processing sequences in Figure 2-12 and 2-13, respectively. The results of these real data sets are however limited only in stacked section to exclude the occurrence of other processing effects that may disturb the ability of deconvolution. The processing sequence is described as follows:

2.3.1 Resampling

Totally 160 raw shot records of 2-D seismic data set 1 and 350 shots of *data set 2* were transferred from a SEG-Y to a Focus/Disco internal data format. Data of *set 1* was resampled to record length of 4 seconds, but this resampling was not applied to the data of set 2.

2.3.2 Geometry setting

Geometry of the survey lines referred in Table 2-3 were assigned to processing software. These were the main parameters used in sorting and stacking.

2.3.3 Editing

Noisy or bad traces and sometime dead traces were killed interactively from the sequence of raw data.

2.3.4 High-pass minimum-phase filtering

High-pass minimum phase filter was applied on the data to filter the low frequency noise and transformed the data to be minimum phase to comply with the deconvolution assumption.

2.3.5 Gain correction

To remove an attenuation effect of all shots, an exponential gain was then applied, following by a spherical divergence correction using the function of time-velocity pairs extracting from representative wells near the tested lines.

2.3.6 Front-end muting

High amplitude firstbreak, refraction events, and guided wave at the shallow time were later removed by truncating proposed mute zone and zeroing.

2.3.7 Periodicity enhancement using *NMO* correction

Assigning the velocity of 1,500 m/s to the *NMO* function. By doing that, all multiple curvatures were lined up and shown repetitive characteristic for all given non-zero offset ranges.

2.3.8 Predictive deconvolution (*PDC*)

By using the optimum parameters in Figure 2-12 and 2-13 with designing guideline in Table 2-4, all shot records of data set 1 and 2 were deconvolved and multiples were theoretically removed from the data. Not only was multiple suppressed, but also resolution of the seismic data was comparatively increased.

2.3.9 Differential *NMO* correction (*DNMO*)

After *PDC*, *NMO* correction was removed subsequently to reverse all seismic reflectors back to the place that they had ever been (Focus reference manual, 1994).

2.3.10 Bandpass filtering.

A band-pass filter was again applied to remove high frequency noise generated from deconvolution process.

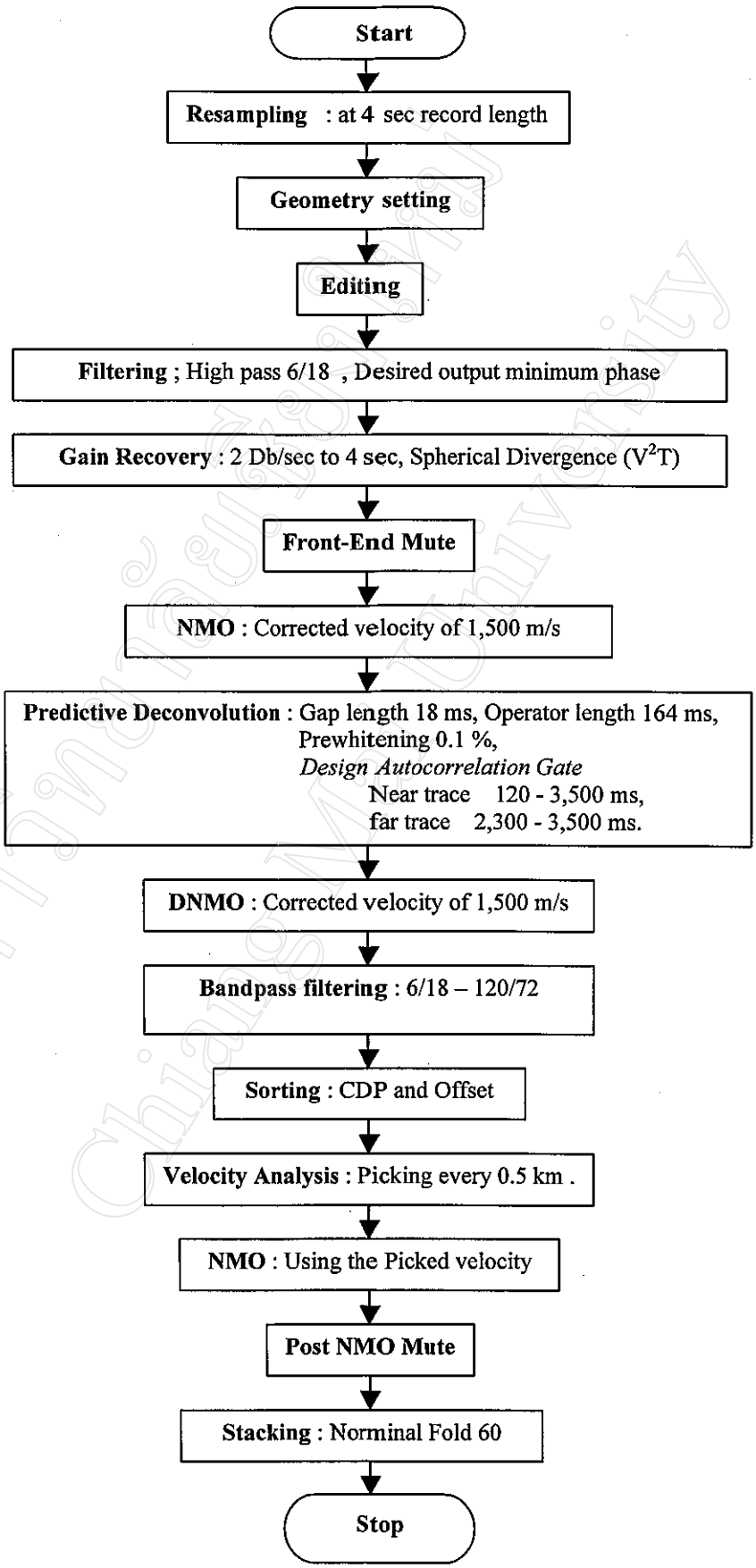

Figure 2-12 Flow of processing sequence of 2-D seismic *data set 1*.

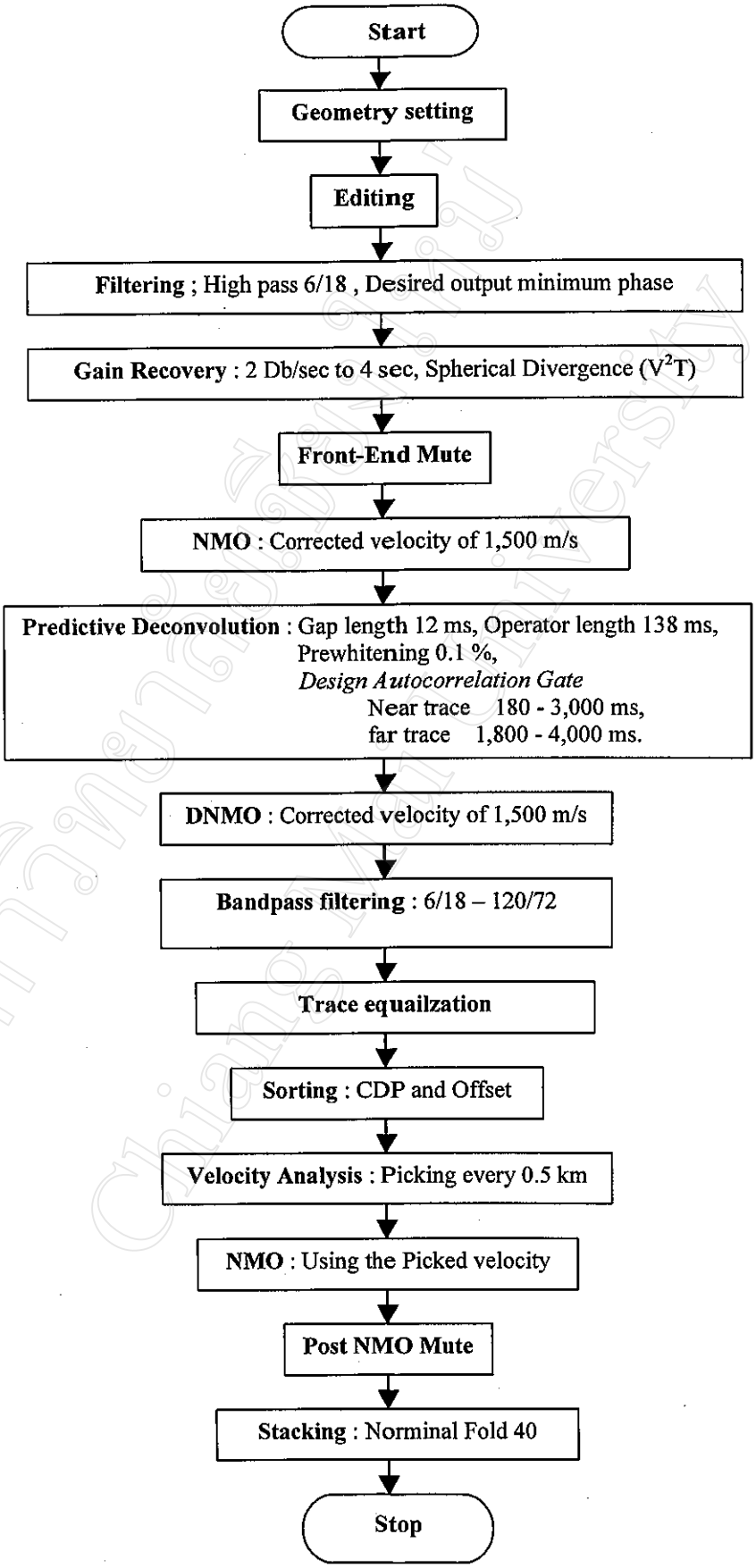

Figure 2-13 Flow of processing sequence of 2-D seismic *data set 2*.

Table 2-4 Predictive deconvolution parameters used in this research comparing with other authors.

	Autocorrelation gate(G)	Gap length (α)	Operator length (n)	Prewhitening (ε)
Yilmaz (1987).	$\geq 8\,n$ (below first break and exclude incoherent noise at deeper time)	At 1st or 2nd zero crossing.	Including the isolated energy packet in the autocorrelation	0.1 – 1 %
Krebes (1989).	-	At 2nd zero crossing	-	0.1 – 1 %
Russell (1990).	$5 - 10\,n$ (Usually 60 – 120 ms for land and ~300 – 2,400 ms for marine.	Vary between 1st and 2nd zero crossing and sometime equal to two-way time of water-bottom multiple	Including the zone of second energy in the autocorrelation and sometime combine with α length	0.01 – 1 %
Tanner (1995).	≥ 6 - $10\,n$	Maximum autocorrelation lag	In front of the actual multiple wavelet and its side lope	-
Jakubowicz (1993).	-	At 2nd zero crossing	Longer than the period of any multiples that are required for removing.	0.01 – 1 %
This research (1998).	Below first break and exclude incoherent noise at deeper time	At 2nd zero crossing.	Compromising between, (1) period which longer than length of existing strong multiple on auto correlation, (2) length which gives best performance derived from testing parameter, and (3) at least 2 times of two-way time of seafloor multiple.	0.1 % or default

2.3.11 Trace equalization

All-offset traces of all shots were averaged to yield the equalization of energy of all traces. This was not applied to data set 1 since its energy was not much differed by offset.

2.3.12 Sorting

All shots were sorted to common depth point (*CDP*) gathers with nominal 60 folds for *data set 1* and nominal 40 folds for *data set 2* based upon a predefined geometry.

2.3.13 Velocity analysis

Velocity analysis was carried out at each 80 *CDP* locations. All velocity functions were calculated and used for the *NMO* correction before stacking.

2.3.14 *NMO* correction

NMO correction of hyperbolic reflection events at certain *CDP* gathers were corrected in *CDP* domain by using time-velocity functions derived from the previous velocity analysis.

2.3.15 Post *NMO* mute

NMO correction made some lower frequencies stretch, therefore the post *NMO* mute was a process to solve this problem. The data was muted at every 40 *CDP* locations.

2.3.16 Stacking

This aims to form a normal stacked (*NSTK*) section with a higher signal to noise ratio. Summing of traces together in each *CDP* gathers results in a stacked trace for each gathers. These stacked traces were displayed horizontally to represent each *CDP* station on seismic section.

Processing results of the two 2-D data sets as three different normal stacked sections, amplitude spectra and frequency spectra are presented and discussed in Chapter 3.